Direct Utilization of Lignite Coal in a Co-CeO_2/YSZ/Ag Solid Oxide Fuel Cell

N. Kaklidis[1], I. Garagounis[2,3], V. Kyriakou[2,3], V. Besikiotis[4], A. Arenillas[5], J.A. Menéndez[5], G.E. Marnellos[1,2,*] and M. Konsolakis[6,]**

[1]*Department of Mechanical Engineering, University of Western Macedonia, GR-50100 Kozani, Greece*

[2]*Chemical Process & Energy Resources Institute, Centre for Research & Technology Hellas, GR-57001 Thermi, Thessaloniki, Greece*

[3]*Department of Chemical Engineering, Aristotle University of Thessaloniki, University Box 1517, Thessaloniki 54124, Greece*

[4]*Department of Chemistry, Center for Materials Science and Nanotechnology, University of Oslo, FERMiO, Gaustadalleen 21, NO-0349 Oslo, Norway*

[5]*Instituto Nacional del Carbon, Apartado 73, 33080 Oviedo, Spain*

[6]*School of Production Engineering and Management, Technical University of Crete, GR-73100 Chania, Crete, Greece*

To whom correspondence should be addressed

***Corresponding author. E-mail:** gmarnellos@uowm.gr **(G.E. Marnellos)**

****Corresponding author. E-mail:** mkonsol@science.tuc.gr **(M. Konsolakis); Tel.: +30 28210 37682; Web:** www.tuc.gr/konsolakis.html

ABSTRACT

The feasibility of employing lignite coal as a fuel in a Direct Carbon Fuel Cell (DCFC) of the type: lignite|Co-CeO_2/YSZ/Ag|air is investigated. The impact of several parameters, related to anodic electrode composition (20, 40 and 60 wt.% Co/CeO_2), cell temperature (700-800 °C), carrier gas composition (CO_2/He mixtures), and total feed flow rate (10-70 cm^3/min), was systematically examined. The effect of molten carbonates on DCFC performance was also investigated by employing a eutectic mixture of lithium and potassium carbonates as carbon additives. In the absence of carbonates, the optimum performance (~~17~~ 10 $mW.cm^{-2}$ at 800 °C), was achieved by employing 20 wt.% Co/CeO_2 as anodic electrode and pure CO_2 as purging gas. An inferior behavior was demonstrated by utilizing He instead of CO_2 atmosphere in anode compartment and by increasing purging gas flow rate. Carbonates infusion into lignite feedstock resulted in a further increase of maximum power density up to 32%. The obtained findings are discussed based also on AC impedance spectroscopy measurements, which revealed the impact of DCFC operating parameters on both ohmic and electrode resistances.

Keywords: Direct Carbon Fuel Cells; lignite fuel; Co/CeO_2 anode; carbonates

1. INTRODUCTION

Coal is by far the most abundant, economic and widely distributed fossil resource. Presently it accounts for more than 30% of the global energy consumption, indicating its primary role in the sector of energy consumption [1]. Nowadays, carbon conversion to energy is mainly achieved in conventional coal-fired plants. However, several crucial issues, related to the thermodynamically restricted low efficiency of the conventional thermal cycles and the increased emissions of environmentally harmful gases produced per MWh, render this process inadequate for a sustainable future. In this regard, the development of novel technologies for efficient and clean coal energy production is of vital importance toward a sustainable energy economy [2-9 ~~2, 3~~].

A direct carbon fuel cell (DCFC) converts the chemical energy of solid carbon directly to electricity at efficiencies well exceeding those of a coal-fired power plant [4]. DCFCs are unique in that because this energy conversion is occurring, without the need of an external gasification process [5]. Potential sources of carbon fuel include coal, coke, graphite, municipal solid wastes (MSW) and other bio-based carbonaceous materials, such as rice hulls, nut shells, corn husks, grass, and wood. These fuels are cheap, abundant, and readily available; therefore, the widespread application of DCFCs does not require a radical change of the existing infrastructure, in contrast to other types of fuel cells. DCFCs have several advantages compared to conventional power plants and gaseous fuelled Solid Oxide Fuels Cells (SOFCs) [6-8]. Firstly, the solid fuel can easily be transported and stored with minor losses, and it can be widely obtained from coal, coke, biomass or even solid wastes [6]. Moreover, its theoretical electrical efficiency is close to 100% due to no entropy change of carbon oxidation [7]. Finally, the direct oxy-combustion of carbon to carbon dioxide can result in a more convenient pathway for an efficient and feasible CO_2 capture [9].

The operating principle of DCFCs based on SOFC configuration is the electrochemical oxidation of carbon by oxygen anions (O^{2-}) transported from the air-exposed cathode through the solid electrolyte to the anode electrode, producing CO_2 (reaction (1)) and CO (reaction (2)). Secondary reactions can also take place on the DCFC anode, including the non-electrochemical Boudouard reaction [10] (reaction (3)) and the further electrochemical oxidation of *in situ* produced CO to CO_2 (reaction (4)).

$$C + 2O^{2-} \rightarrow CO_2 + 4e^- \quad (1)$$

$$C + O^{2-} \rightarrow CO + 2e^- \quad (2)$$

$CO_2 + C \rightarrow 2CO$ (3)

$CO + O^{2-} \rightarrow CO_2 + 2e^-$ (4)

Reactions (1) and (2) are notably hindered by the limited solid carbon/solid electrolyte-electrode interface interactions. However, carbon delivery to the anode active electrochemical zone can be significantly improved by the high carbon fluidity provided by the infusion of a molten carbonate eutectic mixture into the carbon feedstock. In the presence of carbonates, the following stoichiometries, along with reactions (1)-(4), can be simultaneously carried out at anode compartment, improving cell performance [11-14]:

$C + 2CO_3^{2-} \rightarrow 3CO_2 + 4e^-$ (5)

$C + CO_3^{2-} \rightarrow CO + CO_2 + 2e^-$ (6)

$2C + CO_3^{2-} \rightarrow 3CO + 2e^-$ (7)

To date various carbons have been tested as fuels in DCFCs in order to reveal their efficiency as energy carriers. It has been found that their physicochemical, electrical and structural characteristics notably affect their electrochemical reactivity and as a consequence the performance and lifetime of the DCFCs [10, 15-18]. However, as recently reviewed [3] the most common fuel in DCFCs applications is carbon black. Thus, the employment of other types of readily available and cheaper carbon sources would be highly desirable. Taking into account the abundance and the low cost of lignite coal, its employment as feedstock in DCFCs constitutes a highly desirable and efficient way for energy generation from this fuel resource. Furthermore, given that each carbon type has its own physicochemical characteristics which greatly affect the electrochemical performance [18], it would be of significant importance to gain insight into the impact of basic operational parameters on a lignite-fed DCFC.

Lastly, although ceria-based materials, combined with transition metals (e.g. Co, Cu), exhibit adequate electronic conductivity, high oxygen storage capacity and excellent electrocatalytic activity toward the direct electro-oxidation of hydrocarbons in SOFCs, their utilization as anodes in DCFCs is limited [19]. Indeed, Cu and/or Co-Ceria materials offer an interesting combination of electronic conductivity and electrocatalytic activity in direct hydrocarbon fed SOFCs and therefore they could be promising anodes in DCFCs [20]. In a similar manner in our recent study related to the steam reforming of iso-octane over mono- and bi-metallic Cu-Co/CeO_2 catalysts, it is shown

that Co/Ceria composites with a Co content of about 20 wt.% exhibit the optimum characteristics in terms of catalytic activity and carbon tolerance [21].

To this end, the present study aims to assess the potential of direct utilization of lignite coal in a Direct Carbon Fuel Cell (DCFC) of the type: lignite|Co-CeO_2/YSZ/Ag|air. The impact of several parameters related to anodic electrode composition, operation temperature, carrier gas composition and flow rate as well as to the addition of carbonates, was examined. The obtained results are mainly interpreted on the basis of AC impedance spectroscopy, which revealed the impact of anodic electrode composition and DCFC operating parameters on cell resistances.

2. MATERIALS AND METHODS

2.1 Materials synthesis

The wet impregnation method was used in order to prepare Co/CeO_2 catalysts with different cobalt loadings (20, 40, 60 wt.%), which were employed as anodic electrodes. The $Ce(NO_3)_3 \cdot 6H_2O$ precursor (99%, Sigma-Aldrich) was initially dissolved in distilled water and heated to 125 °C, under stirring, till all the water evaporated. The resulting sample was dried for 16 h at 110 °C, and then calcined for 2 h at 600 °C. The corresponding stoichiometric quantity of $Co(NO_3)_2 \cdot 6H_2O$ (99%, Sigma-Aldrich) precursor was dissolved in distilled water and impregnated onto the calcined CeO_2 support in order to yield the desired metal loading. The drying procedure for this solution and the calcination of the resulting powder was identical to that described for the ceria support.

2.2 Fuel characterization

In the present study lignite coal was employed as fuel. The coal was chemically analyzed by means of elemental analysis (C, H, N, S and O wt.% content) in LECO CHNS-932 and LECO VTF-9000 analyzers. Proximate analysis (volatiles, ash and moisture content) was carried out using the LECO TGA-601 equipment. Ash composition was determined by X-ray fluorescence (XRF) in a Bruker SRS 3000 device. Lignite was also characterized by Fourier transform infrared spectroscopy (FTIR) in a Nicolet FTIR 8700 with the diffuse reflectance module Smart Collector. A high-sensitivity detector MCT-A of mercury cadmium telluride was used. The data were recorded between 4000-650 cm^{-1}, using 100 scans and a resolution of 4 cm^{-1}.

Finally, the reactivity of the lignite coal was also characterized by thermogravimetric (TG) analysis. Samples were heated up to 1000 °C with a rate of 10 °C/min in a thermobalance (Q5000 IR, TA

Instruments). The weight loss profile was recorded with increasing temperature, under both inert (N_2) and reactive (CO_2) atmosphere at a constant flow rate of 20 cm^3/min.

2.3 DCFC fabrication and testing

The fuel cell experiments were carried out in a reactor cell (Figure 1) consisting of an YSZ tube (CERECO) with 1.2 mm thickness, closed flat at its bottom end. The cathode was deposited on the outside wall of the closed end of the YSZ tube, prepared from a silver paste (05X Metallo-organic AG RESINATE) after calcination for 2 h at 850 °C in stagnant air, with a heating rate of 4 °C/min. The working (anodic) electrode was prepared from a Co/CeO_2 powder, mixed with ethylene glycol at a 1:2 weight ratio. The solution, consisting from powder catalyst dissolved in ethylene glycol, was heated at about 200 °C (boiling point of ethylene glycol= 197.3 ^oC) and stirred at 400 rpm until half of its volume was evaporated. The viscous suspension was then deposited, with the aid of a paintbrush, on the inside bottom wall of the YSZ tube. The calcination procedure involved heating, under atmospheric air, to 850 °C for 2 h with a heating rate of 4 °C/min. After calcination, the cell was cooled down to 200 °C, where the anode was reduced in a flow of 30 cm^3/min of H_2 (100 vol.%) for 2 h. In all cases, the amount of the anodic electrode deposited on the YSZ surface was equal to 115 mg, resulting in an apparent electrode area of 1.7 cm^2.

Fuel cell measurements were carried out in the temperature range of 700-800 °C, at atmospheric pressure. In each experiment the cell, loaded either with bare carbon (800 mg lignite) or a carbon/carbonate mixture (800 mg lignite/200 mg carbonates), was initially heated from room temperature to 700 °C at a heating rate of 4 °C/min. In the latter case, lignite was initially diluted in 250 mL of n-hexane and agitated in an ultrasonic device for 15 min before the addition of carbonates mixture. The resulting solution was stirred on a heating plate at 70 °C for 4 h until all the n-hexane evaporated. A gas mixture of CO_2 and He (99.999 % purity, Air Liquide) at various compositions (0, 25, 50, 75 and 100 vol.% CO_2 in He) was employed as purging gas in the anode chamber, whereas the cathode was exposed to atmospheric air. The flow rate of carrier gas was controlled by mass flow meters (Tylan FM 360) and introduced into the reactor cell at a rate of 10-70 cm^3/min. The cell voltage and developed electrical current were monitored by means of digital multi-meters (RE60-69) and the external resistive load was controlled by a resistance box (Time Electronics 1051).

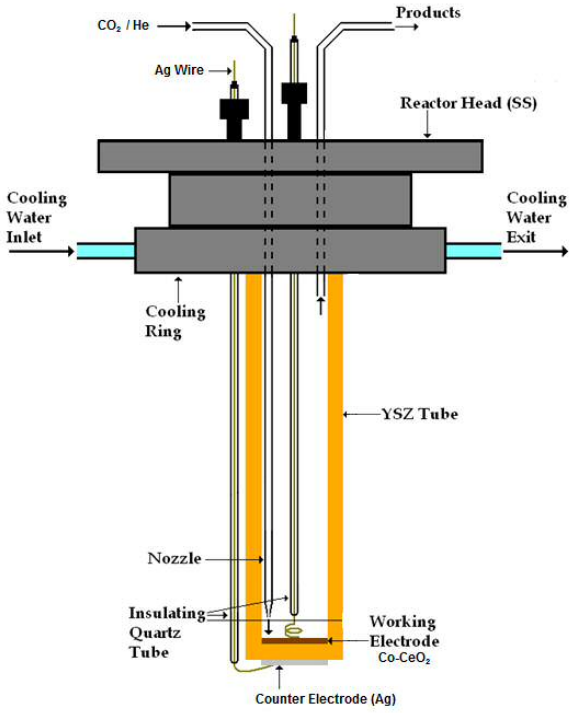

Figure. 1: Schematic illustration of the cell reactor.

2.4 Electrochemical Impedance Spectra (EIS) measurements

The electrochemical impedance spectra were obtained under open circuit conditions in the frequency range between 0.1 Hz and 1 MHz with an amplitude of 30 mV RMS, using the Versa Stat 4 electrochemical workstation by Princeton Applied Research and the corresponding software (Versa Studio) for data processing. Analysis of the effluents was performed by an on-line Gas Chromatograph (SRI 8610B) equipped with a Molecular Sieve 5A and a Porapak Q columns.

The impedance data were validated with a Kramers-Kronig transform program [22] and analyzed with the software package "Equivalent Circuit for windows" [23]. The impedance spectra were fitted to $R_{bulk}(R_2Q_1)(R_3Q_2)$ equivalent circuit with chi-squared (χ^2) values being below 10^{-6}. Here, R_{bulk} is the ohmic resistance, mainly from the electrolyte. The $(R_2Q_1)(R_3Q_2)$ represent the deconvoluted values of the low frequency dispersion in the Nyquist plot. The (R_iQ_i) denotes a resistor and a constant phase element (CPE) in parallel. The pseudo-capacitances C_1, C_2 were calculated from Q_1, Q_2 using the following equation:

$$C_i = Y_i^{\frac{1}{n_i}} R_i^{\frac{1}{n_i}-1} \qquad (8)$$

Y_i and n_i define the complex admittance of the CPE given by $Y_{CPE} = Y_i(j\omega)^{n_i}$, where ω is the angular frequency and $j = \sqrt{-1}$ [~~16~~ 24]. The $R_{bulk,}$ (R_2Q_1), and (R_3Q_2) are in series with each other. The sum of R_2 and R_3 is the electrode resistance, $R_{electrode}$.

2.5 Electrical conductivity measurements

Direct Current Four Point (DC4P) measurements were conducted under controlled atmosphere in order to estimate the electrical conductivity of anode materials. Sufficient quantity of 20 wt.% Co/CeO_2 powder, which employed mainly as anode, was uniaxially pressed into Ø25mm pellet with 1.5 tn load and annealed at 850^{o}C/2h in order to achieve some mechanical properties. Subsequently, the pellet was cut in rectangular rod and four Pt-wire electrodes were attached to the rod, gluing them with Pt paste. The rod was then inserted into a proper stand of controlled atmosphere consisted of a sample holder, a quartz tube, quick connectors for the atmosphere control, four Pt wires for the connections to the power supply, a digital multimeter and a K-Type thermocouple.

Firstly, the temperature increased at 850 ^{o}C for 2h under atmospheric air flow in order to obtain a good adhesion of the Pt-contacts. The system was cooled physically and when it reached 200 ^{o}C a flow of 100 vol.% H_2 at 20 cm^3/min was fed into the system until it reached 50 ^{o}C. Then, the flow switched to He and the temperature increased to 700 ^{o}C with a ramp rate of 4^{o}C/min. Measurements were performed at 700, 750 and 800 ^{o}C by providing 1 mA to the external Pt wires and measuring the voltage in the inner Pt-wires. Afterwards, the system cooled to 650 ^{o}C and the flow switched to a mixture of 3 vol.% CO in He, in order to obtain conductivity measurements under CO atmosphere.

3. RESULTS AND DISCUSSION

3.1 Chemical properties of lignite fuel

In Table 1 the proximate and ultimate analysis of lignite coal is depicted. The corresponding mineral matter composition is presented in Table 2. It can be seen that lignite coal has a low sulphur (0.8 wt.%) and relatively low ash (17.6 wt.%) content. These low values are desirable in terms of fuel cell performance and durability, since their inhibiting role on DCFC operation has been already acknowledged [15]. Furthermore, the mineral matter analysis of ash (Table 2) indicates that sulphur is mainly inorganic, thus being less reactive. In regard to other components of mineral matter, Si, Ca and Al are mainly identified, as expected. Intermediate amounts of Mg (7.0 wt.%) and Fe (9.3

wt.%) are also determined, whereas mineral matter constitution in Na, P and Ti is essentially negligible.

On the other hand, it is worth mentioning the high volatile matter (ca. 43 wt.%) and high oxygen content (ca. 40 wt.%) of lignite. These characteristics indicate that lignite coal could be a feedstock of choice, since many of the loosely bonded volatiles and oxygen surface groups are expected to be released with increasing temperature. These surface groups along with the active sites of solid carbon residue are very active towards carbon gasification, increasing the reactivity of lignite. The latter is justified below based on thermogravimetric analysis under an inert (N_2) or a reactive (CO_2) atmosphere.

Table 1: Proximate and ultimate analysis of the lignite coal

Proximate Analysis (wt.%)			**Ultimate Analysis (wt.%, dry ash free basis)**				
VM	**Ash**	**Moisture**	**C**	**H**	**N**	**S**	**O**
42.6	17.6	11.7	55.1	3.6	0.9	0.8	39.7

Table 2: Mineral matter composition (wt.%) of ash in the lignite coal

Na_2O	MgO	Al_2O_3	SiO_2	P_2O_5	K_2O	CaO	TiO_2	Fe_2O_3	SO_3
0.0	7.0	18.3	25.4	0.1	0.2	22.8	0.4	9.3	15.6

In Figure 2 the FTIR spectrum of the lignite coal is presented. The broad band in the 3200-3600 cm^{-1} region arises from the hydroxyl, carboxyl and phenol groups present in lignite coal. The band in the 1600-1750 cm^{-1} region can be assigned to C=O vibration in aldehydes-, ketones- and ester-like groups. The appearance of these bands are in agreement with the high oxygen content of the lignite coal (ca. 40 wt.%, Table 1). The rest of the bands can be attributed to C-H stretching vibration in aliphatic and aromatic compounds.

Figure 2: FTIR spectrum of lignite coal.

The reactivity of the lignite coal was evaluated by thermogravimetric analysis. Figure 3 depicts the weight loss evolution upon temperature increase under an inert (N_2) or a reactive (CO_2) atmosphere. The weight loss profiles in the two different atmospheres are very similar up to 700 °C; CO_2 does not interact with lignite coal at temperatures lower than 700 °C resulting in almost parallel weight loss profiles under N_2 and CO_2 atmosphere. At temperatures lower than 100 °C a low weight loss is observed, which is in accordance with the moisture content of lignite coal (ca.12 wt.%, Table 1). The weight loss between 300-700 °C can be attributed to the breakage of labile bonds in the coal structure and the evolution of the lignite volatiles. At higher temperatures (i.e. >700 °C) a very low weight loss was recorded under inert atmosphere (N_2); this can be due to the reorganization of the carbonaceous matter which is accompanied by some CO and H_2 evolution. However, when the sample is exposed to CO_2, the carbonaceous matter of the lignite (i.e. lignite char) reacts with CO_2, resulting in a significant weight loss at high temperatures, where the reverse Boudouard reaction is favored. These reactions occur till the complete consumption of the remaining carbonaceous matter. At 900 °C there is no char left and only the residual mineral matter is present (ca. 17 wt.%, Table 1), which is non-reactive and therefore no further weight loss is recorded (Fig. 3).

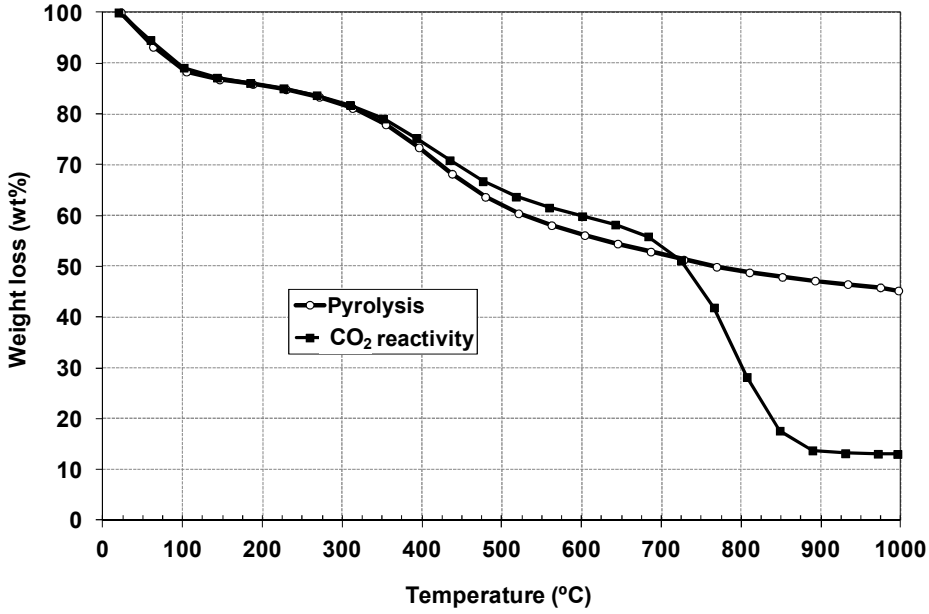

Figure 3: Weight loss profiles of the lignite coal with increasing temperature in an inert (N_2) and a reactive (CO_2) atmosphere

3.2 DCFC performance

3.2.1 Effect of anode composition on fuel cell performance under He flow

Figure 4 depicts the effect of anode composition (20, 40 and 60 wt.% Co/CeO_2) on DCFC characteristics at three different temperatures, 700, 750 and 800 °C, under He flow, in terms of cell voltage, developed current density and power density. As it can be observed, the anode composite with 20 wt.% Co loading demonstrated the best performance at all the examined temperatures, resulting in a maximum power density of 2.35, 4.2 and 6.15 ~~4.00, 7.15, and 10.45~~ mW.cm^{-2} at 700, 750 and 800 °C, respectively. Concerning the developed Open Circuit Voltage (OCV), a clear increase in the absolute OCV values is observed with increasing temperature, while OCV slightly increases by varying the anode composition. OCV absolute values of 930, 938 and 940 mV are recorded at 800°C for 20, 40 and 60 wt.% Co/CeO_2 anodes, respectively, which are higher to those reported for 20 mol% Yttria-doped Ceria (0.85 V) and 40 mol% Gadolinia-doped Ceria (0.91 V) Ni (2 wt.%) infiltrated anodes in DCFC studies employing activated coconut charcoal as fuel [19]. These OCV values are slightly lower to the theoretical voltage (1.0 V) expected for carbon oxidation reaction [19]. However, theoretical OCV assumes reversible electrochemical reactions on both electrodes, gas-tightness between the anode and cathode chambers, and a completely reversible adsorption/desorption of reactants/products. Nevertheless, under real work conditions, significant deviations from the ideal state would be expected [19]. Furthermore, a linear dependence of cell

voltage on the developed current density is observed; as the operating temperature increases and Co loading decreases, the cell voltage-current slopes decrease resulting in higher power outputs.

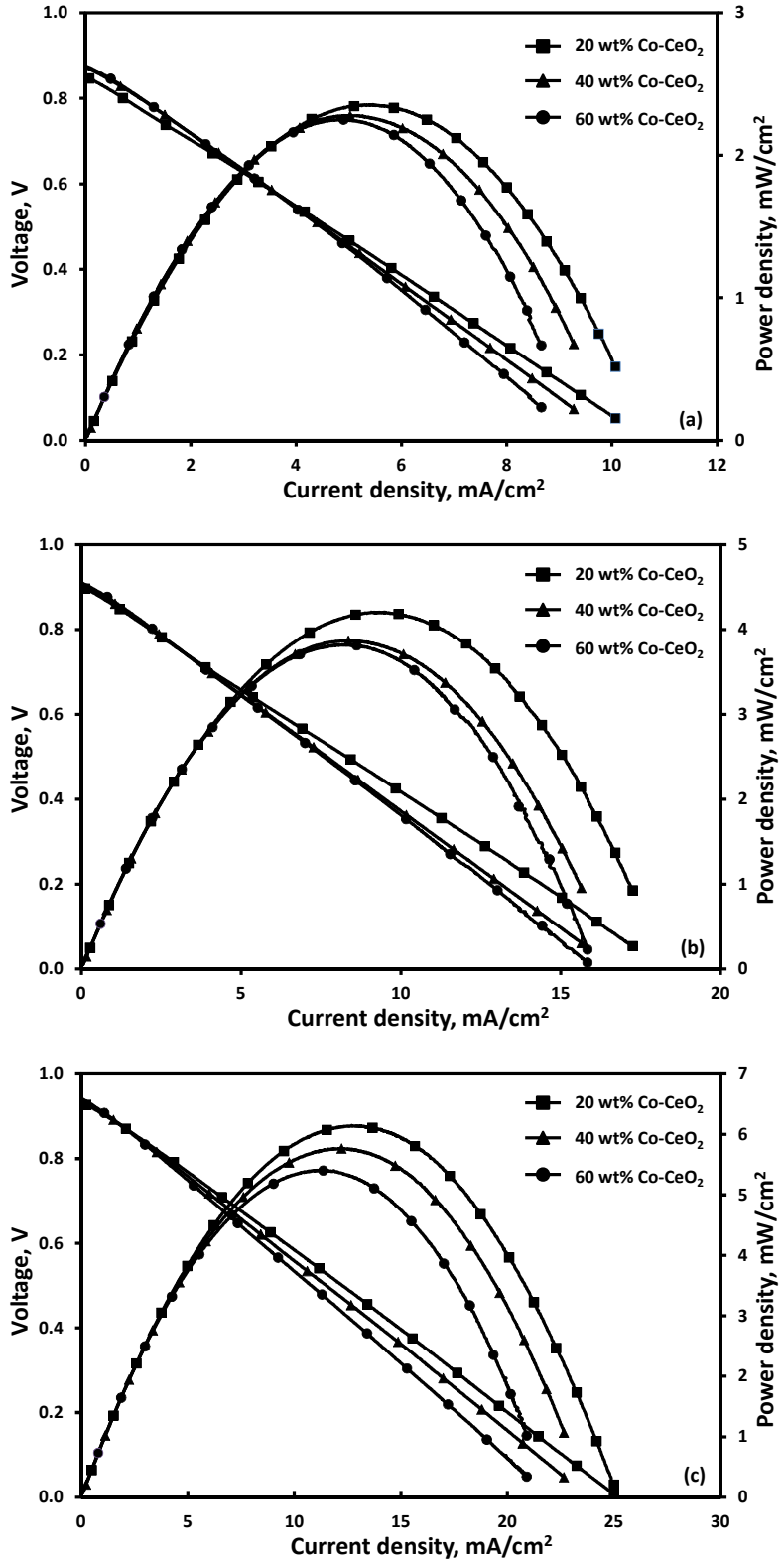

Figure 4: Effect of anode composition on DCFC performance under pure He flow at a) 700 °C, b) 750 °C and c) 800 °C. Feedstock: 800 mg lignite; Carrier gas (100 vol.% He) flow= 30 cm^3/min.

The corresponding open circuit AC impedance spectra at 800 ^{o}C (Figure 5), obtained at conditions identical to those employed in Figure 4c, showed that the ohmic resistance of the cell, substantially decreased by decreasing Co content in Co/CeO_2 composites; ohmic resistance values of 9.8, 8.8 and 6.3 Ω cm^2 are recorded for 60, 40 and 20 wt.% Co, respectively, reflecting the higher achieved power densities obtained in the case of 20 wt.% Co/CeO_2 anode composite. On the other hand, electrochemical impedance spectra modeling, reveals that the corresponding electrode resistance is less influenced by the anode composition; electrode resistance values of 6.5, 4.8 and 6.1 Ω cm^2, are observed for 60, 40 and 20 wt.% Co, respectively. Given that the cathode and electrolyte materials as well as the anodic and cathodic atmospheres are identical in all the examined cases, the corresponding alterations in the AC impedance spectra can be attributed to the anode composition. Since the electrode resistance depicted by the two arcs in EIS reflects the electrode kinetics and mass transfer limitations, the observed behavior can be possibly ascribed to slight modifications in electro-catalytic activity upon altering the Co content.

The values of the pseudo-capacitances are ranged from 0.2 to 4.5 ~~20~~ mF.cm^{-2} for the high frequency arc and 13 to 32 mF.cm^{-2} for the low frequency arc, which are typically assigned to the electro-oxidation of lignite and/or *in situ* formed CO at the triple phase boundary (tpb) as well as to the adsorption/desorption and diffusion of reactive species on the anode. In this regard, Kulkarni *et al.* [25] studied the performance of 2 wt.% Ru-infiltrated $La_{0.3}Sr_{0.7}Ti_{0.93}Co_{0.07}O_3$ (LSCT) as anode materials in DCFC cells of the type Ru-LSCT/YSZ/LSCF, fed with carbon black (Vulcan XC-72, Cabot Corp.) at 800 ^{o}C and employing pure N_2 as purging gas. They reported maximum power density values equal to 25 and 7.5 mW.cm^{-2} for Ru-LSCT and LSCT anodes. In their EIS modeling, capacitance values of 0.3 and 0.2 mF.cm^{-2} for the high and low frequency arcs associated to the charge transfer processes of carbon and CO electro-oxidation and 8 and 1.1 mF.cm^{-2} for the corresponding arcs related to adsorption and diffusion processes, were estimated [25]. These values are of the similar order of magnitude to those reported here, being, however, relatively lower. This deviation can be explained by taking into account the differences in cell materials and fuel type as well as in the equivalent circuit applied in EIS modeling.

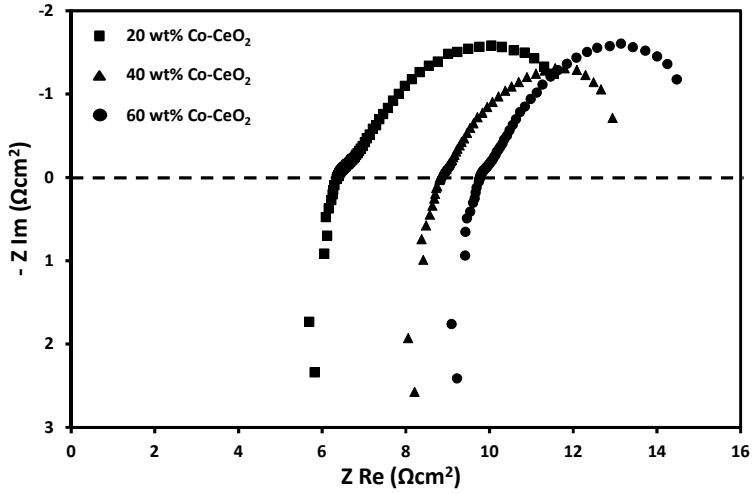

Figure 5: AC impedance spectra at 800 °C for different anode compositions. Feedstock: 800 mg lignite; Carrier gas (100 vol.% He) flow= 30 cm^3/min.

3.2.2 Effect of carrier gas (He or CO_2) on fuel cell performance.

The effect of carrier gas (100 vol.% He or CO_2) on DCFC performance, employing 20 wt.% Co/CeO_2 as anode, at 700, 750 and 800 °C and the corresponding AC impedance spectra are depicted in Figure 6. The results clearly indicate the enhanced DCFC performance in the case of CO_2 flow (+65% at 800 °C), which is also reflected on the higher obtained absolute OCV values compared to pure He flow. A maximum power density of 3.30, 6.19 and 10.05 $mW.cm^{-2}$ at 700, 750 and 800 °C, respectively, is obtained under CO_2 flow, compared to 2.35, 4.20 and 6.15 $mW.cm^{-2}$ under He flow.

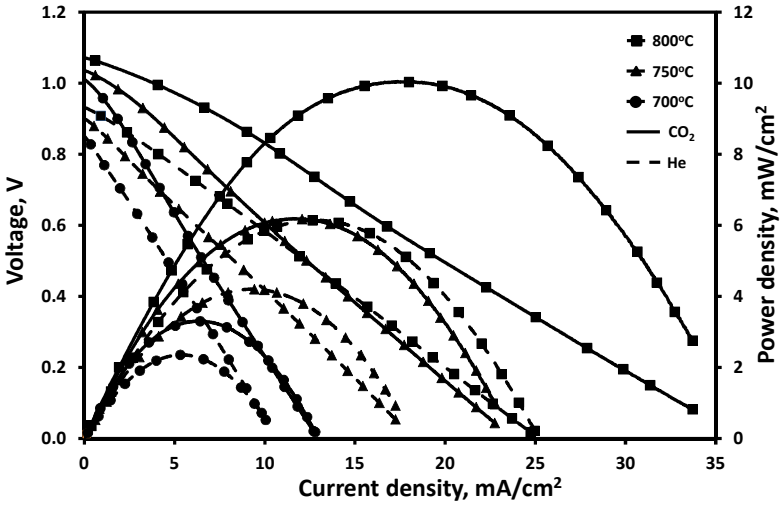

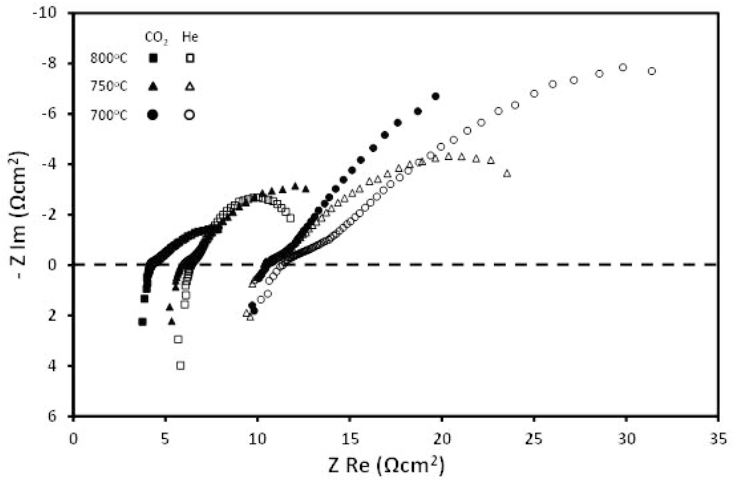

Figure 6: Effect of carrier gas (100 vol.% He or CO_2) on DCFC performance at 700-800 °C and the corresponding AC impedance spectra. Feedstock: 800mg lignite; Carrier gas (He or CO_2) flow= 30 cm^3/min

This enhancement can be mainly attributed to the *in situ* formation of CO, through the reverse Boudouard reaction (reaction 3), and its subsequent electro-oxidation at the tpb (reaction (4)). The voltage-current slopes decrease with increasing cell temperature and when using CO_2 instead of He as carrier gas, resulting in an improved DCFC performance. These findings can be further interpreted based on the corresponding open circuit AC impedance spectra in Figure 6. It is obvious that the ohmic resistance of the cell, corresponding to the intercept of the arc with the real axis, is decreased by increasing cell temperature from 10.4 Ω cm^2 at 700 °C to 4.15 Ω cm^2 at 800 °C under CO_2 flow. Concerning the electrode resistance, the values of 33.4, 11.4 and 6.2 Ω cm^2 are obtained at 700, 750 and 800 ^oC, respectively. A similar behavior was observed in the case of He flow; however the corresponding ohmic and electrode resistances were much higher compared to CO_2 flow DCFC operation. These differences are mainly attributed to the presence of excess CO formed under CO_2 flow, which may lead to the partial reduction of Co/CeO_2 anode composite as well as to the better diffusion and faster electro-oxidation kinetics compared to solid lignite (lower $R_{electrode}$).

Assuming that the cathode polarization losses are essentially negligible compared to the ohmic resistance (since metallic Ag was employed as cathode electrode), the anode polarization contribution at 800 ^oC under both He and CO_2 flow is lower than 65-70% of overall cell losses for an average current density of 20-30 $mA.cm^{-2}$ at 0.5 V. This value is higher to that reported for YDC electrodes (30%), indicating the significant limitations originated from the employed anode composites [19].

In this point it should be noted that both ohmic and electrode resistance values calculated from Figures 5 and 6, are of the same order of magnitude to those reported in relevant literature studies [19, 25], being, however, to some extent higher. Kulkarni *et al.* [19] employed 2 wt.% Ni-infiltrated Yttria doped Ceria (20 mol% YDC) and Gadolinia doped Ceria (40 mol% GDC) as anodes in DCFC utilizing YSZ as electrolyte (thickness= 0.45 mm) and activated coconut charcoal as feedstock. The optimum performance was observed for YDC anodes, which offer a maximum power density of ca. 33 and 40 $mW.cm^{-2}$ at 800 ^{o}C, when pure N_2 and 40 vol.% CO_2/N_2 were employed as purging gases, respectively. The ohmic resistance under the presence of both carrier gases was equal to 3.98 Ω cm^2, which is similar to that reported in the present study (4.1 Ω cm^2). The electrode resistances were equaled to 2.82 and 1.23 Ω cm^2, for pure N_2 and CO_2/N_2 flows, respectively, reflecting the positive effect of *in situ* formed CO on cell performance under CO_2 presence [19]. This pronounced effect was attributed to the better diffusion of CO; the Warburg element was much higher under inert atmosphere (1.73 $\Omega.cm^2$) compared to reactive atmospheres (0.1 $\Omega.cm^2$), although all other resistance counterparts were similar at both atmospheres.

The dominant feature in the impedance spectra interpreted in the present study is a small high frequency (HF) arc overlapped with a large arc at low frequencies (LF). The size of both arcs decreases significantly by increasing the cell temperature and by switching the carrier gas flow from He to CO_2. The LF arc is always significantly smaller at inert environment (0.42 Ω cm^2 at 800 ^{o}C, Figure 6) compared to CO_2 atmosphere (1.69 Ω cm^2 at 800 ^{o}C, Figure 6). The opposite behavior is observed for the HF arc, where the corresponding values are equal to 6.31 and 4.56 Ω cm^2 (Figure 6). The corresponding pseudo-capacitance values for the LF arc in the case of He carrier gas is 0.19 $mF.cm^{-2}$, while for CO_2 flow is 28.9 $mF.cm^{-2}$. On the other hand, the pseudo-capacitance values for the HF arc are of the order of 10^{-2} $F.cm^{-2}$, under both He and CO_2 flow.

Taking into account the above observations and the reaction mechanism proposed in [19] for carbon electro-oxidation over YDC under N_2 or CO_2/N_2 flows, it can be argued that the HF arc can be ascribed, apart from a small contribution from cathode, to the electro-oxidation of carbon and the associated physical processes (adsorption/desorption and diffusion of reactive species). The LF arc which is significantly reduces upon utilizing CO_2 as carrier gas, and by increasing the cell temperature, can be ascribed to the electro-oxidation of CO and the corresponding physicochemical processes [19]. Specifically, under He flow the HF arc is slightly modified with temperature and the

capacitance values clearly indicate that the charge transfer reaction (electro-oxidation of carbon) determines the process. In contrary, the LF arc is notably decreased with temperature. Moreover, the capacitance values (~10^{-2} F.cm^{-2}) indicate that the process related to LF arc is equally determined by the electro-oxidation of CO and its adsorption/diffusion. However, under CO_2 flow the HF arc is higher compared to that in He flow, decreasing notably with temperature. The corresponding pseudo-capacitance values imply both charge transfer and diffusion processes. However as the temperature decreases, the pseudo-capacitance values are increased, indicating the major role of mass transfer limitations. The LF arc is significantly smaller compared to that in He-purged cell, whereas it decreases notably with increasing cell temperature, indicating the pronounced role of *in situ* formed CO. Similar AC impedance behavior to that described above has been obtained by C. Munnings *et al.* [26], in a cell using LSCF as anode/cathode electrodes and coconut char as feedstock. The impact of carrier gas (He or CO_2) on ohmic and electrode resistances is further interpreted in following sections.

3.2.3 Effect of carrier gas composition on fuel cell performance

The effect of CO_2 concentration was examined at 750 °C by employing the optimum anode composition (20 wt.% Co/CeO_2) and gasification agent (CO_2). Figure 7 shows the voltage–current density and power density–current density characteristics of the cell as well as the corresponding AC impedance spectra in different CO_2 concentrations. The DCFC performance is almost proportional to CO_2 concentration verifying again the positive contribution of reverse Boudouard reaction ($CO_2 + C \rightarrow 2CO$), on cell characteristics. A maximum power density, P_{max}, of about 5.88 ~~10~~ mW.cm^{-2} is obtained with 100 vol.% CO_2 instead of ~3.52 ~~6~~ mW.cm^{-2} with 25 vol.% CO_2. The obtained DCFC performance is well correlated with the corresponding open circuit AC impedance results. It can be seen that the ohmic resistance ~~ASR~~ depends strongly on the gaseous environment, as already indicated in the previous section. This could probably be attributed to the altered redox properties of the anodic electrode affected by the surplus *in situ* formed CO, as the CO_2 concentration is increased (reaction (3)). Specifically, as the CO_2 concentration decreases, the ohmic resistance increases (from 6.5 Ω cm^2 at 100 vol.% CO_2 to 10.6 Ω cm^2 at 25 vol.% CO_2). A similar trend is also obtained for the electrode resistance, $R_{electrode}$, attributed to the anode chemical, electrochemical and physical processes (adsorption/desorption, diffusion). This behavior could be explained by considering the additional amount of CO formed upon increasing CO_2 concentration, which in turn contributes to decreased mass transfer limitations and faster electrode kinetics.

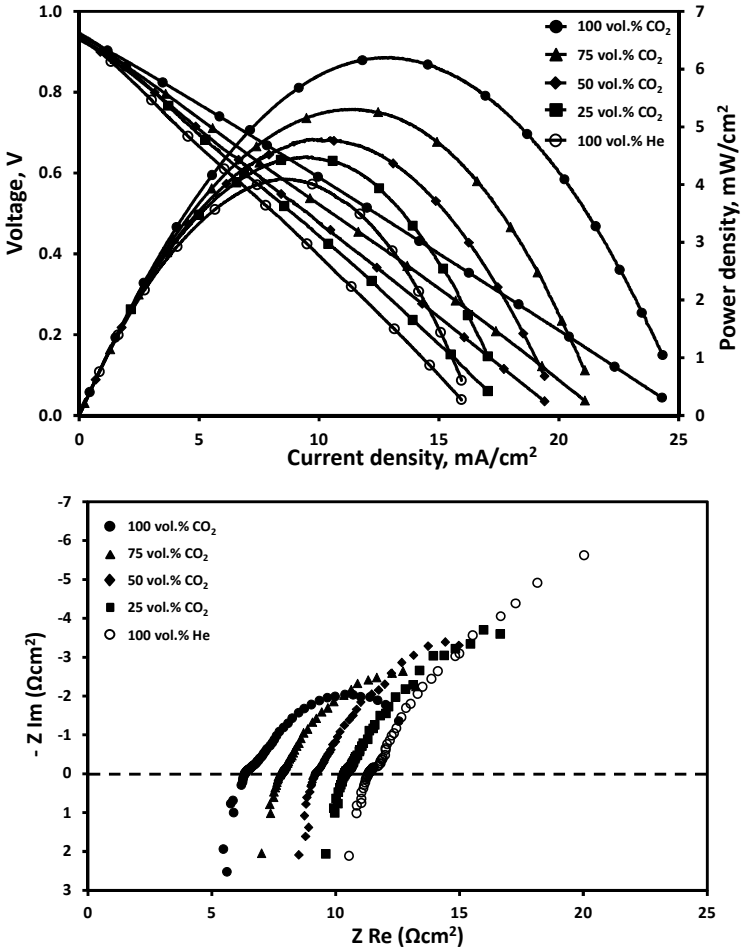

Figure 7: Effect of carrier gas composition on DCFC performance at 750 °C and the corresponding AC impedance spectra. Feedstock: 800mg lignite; Carrier gas (CO_2/He mixtures) flow= 30 cm^3/min.

3.2.4 Effect of carrier gas flow rate on fuel cell performance

The effect of carrier gas (100 vol.% CO_2) flow rate on DCFC performance at 750 °C and the corresponding AC impedance spectra are presented in Figure 8. It is evident that the DCFC performance is inversely proportional to the total flow rate of the carrier gas in the anode chamber. The optimum performance is obtained with 10 cm^3/min and is equal to 7.65 $mW.cm^{-2}$. Under similar conditions much lower power density values are obtained by increasing the flow rate up to 70 cm^3/min (3.59 $mW.cm^{-2}$). The latter is related to the higher residence time leading to higher formation rates of CO through the reverse Boudouard reaction, a fact which is verified by the measured CO formation rates. The open circuit AC impedance spectra showed that the ohmic resistance, substantially increased by increasing gas flow rate from 4.37 Ω cm^2 at 10 cm^3/min to 8.23 Ω cm^2 at 70 cm^3/min. Electrode resistance, $R_{electrode}$, also increased substantially with the flow

rate. These modifications upon changing the flow rate of carrier gas can be interpreted by taking into account the impact of excess CO on the surface/redox properties of the anode and on its improved diffusion and fast electro-oxidation kinetics.

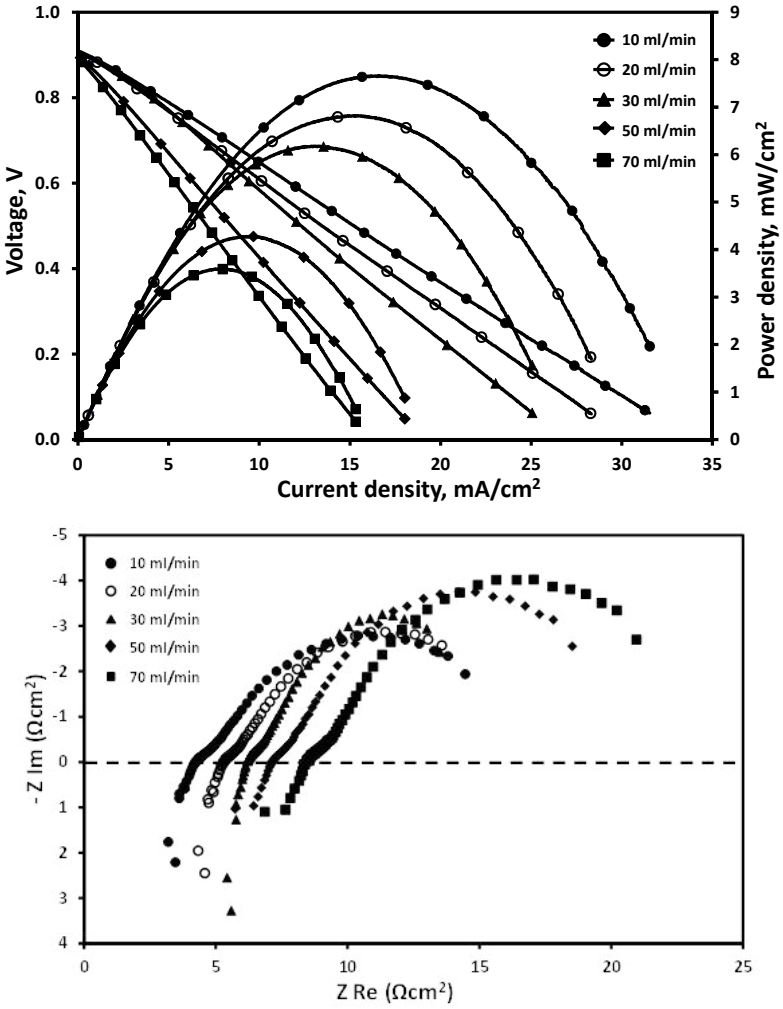

Figure 8: Effect of carrier gas (CO_2) flow rate on DCFC performance at 750 ^oC and the corresponding AC impedance spectra. Feedstock: 800 mg lignite; Carrier gas (100 vol.% CO_2) flow= 10-70 cm^3/min.

3.2.5 Effect of molten carbonates infusion on fuel cell performance

A eutectic mixture of lithium and potassium carbonates (62 mol% Li_2CO_3 + 38 mol% K_2CO_3) were mixed with lignite at a carbon/carbonate weight ratio of 4:1, in order to investigate the impact of molten carbonate electrolyte on DCFC performance. Figure 9 depicts the impact of carbonates on cell voltage, developed current density and power density at 700, 750 and 800 °C under CO_2 flow and the corresponding AC impedance spectra. The pronounced effect of carbonates infusion into lignite is evident in the whole temperature range investigated. Specifically, the addition of

carbonates led to a 32% increment of the power at 800 °C, compared to that obtained in the absence of carbonates. However, lower absolute OCV values are in general developed in the presence of carbonates. Moreover, the anode polarization contribution to the overall cell losses is slightly improved (~ < 60%,) compared to that obtained in the absence of carbonates (~ < 70%).

In relation to the impact of carbonates on OCV values it should be noted that the possibility of multiple reactions taking place in anodic chamber as well as at anode/electrolyte and anode/fuel interfaces, makes difficult to predict equilibrium oxygen concentration and thus the OCV. In this regard, it has been observed that OCV can be notably affected by fuel type, temperature and operated conditions [18]. Reactions (1)-(4) can be accounted for the determination of oxygen concentration in DCFCs. In the presence of carbonates reactions (5)-(7) should be also considered. In our previous study related to the impact of fuel type and carbonates on DCFC performance, it was observed that OCV values followed in general the same trend with the CO formation rate; absolute OCV values are increased with the operating temperature and when carbonates infused in the carbon feedstock [18]. In the present study, however, a slight decrease on OCV is observed in the presence of carbonates, despite their pronounced influence on CO formation (Figure 9). It can be therefore assumed that the equilibrium oxygen concentration in the co-presence of lignite and carbonates is equally determined by fuel characteristics and anode/fuel reactions as well as by the presence of carbonates.

The open circuit AC impedance spectra (Figure 9) are in accordance with the observed cell characteristics. The ohmic resistance is significantly decreased with the addition of carbonates in the lignite feedstock, *e.g.*, from 10.4, 5.8 and 4.1 Ω cm^2 with bare lignite to 6.9, 4.7 and 3.5 Ω cm^2 in the co-presence of carbonates, at 700, 750 and 800 ^oC, respectively. As can be seen, this enhancement is more pronounced at lower temperatures since the improvement of ohmic and electrode resistances is more obvious. Moreover, from the deconvolution of the impedance spectra at 750 °C it is evident that the electrode resistance $R_{electrode}$, decreased from 19.8 Ω cm^2 to 4.4 Ω cm^2 with the addition of the carbonates. In addition, the pseudo-capacitance values are notably decreased in the presence of carbonates from 59 to 0.35 $mF.cm^{-2}$ and from 52 to 20 $mF.cm^{-2}$ for the high and low frequency arcs, respectively. Therefore, based on the analysis performed in Section 3.2.2, the HF arc in the presence of carbonates is determined by the electro-oxidation of carbon. Pseudo-capacitance values increases with temperature, reflecting the higher role of diffusion processes upon temperature increase. On the other hand, the pseudo-capacitance values for the LF

arc are of the order of 10^{-2} F.cm^{-2}, both in the presence and absence of carbonates, indicating that the electro-oxidation process contributes equally with the physical (adsorption, desorption and diffusion of reactive species) processes, in relation to LF arc. Interestingly, the enhanced DCFC performance in the presence of carbonates is accompanied by higher CO formation rates, as also observed in [18]. This indicates that the beneficial effect of carbonates can be attributed, apart from the high fluidity of lignite in anode side and thus its improved diffusion, to the additional amount of CO formed through the reactions (6) and (7) and its subsequent electro-oxidation at the tpb.

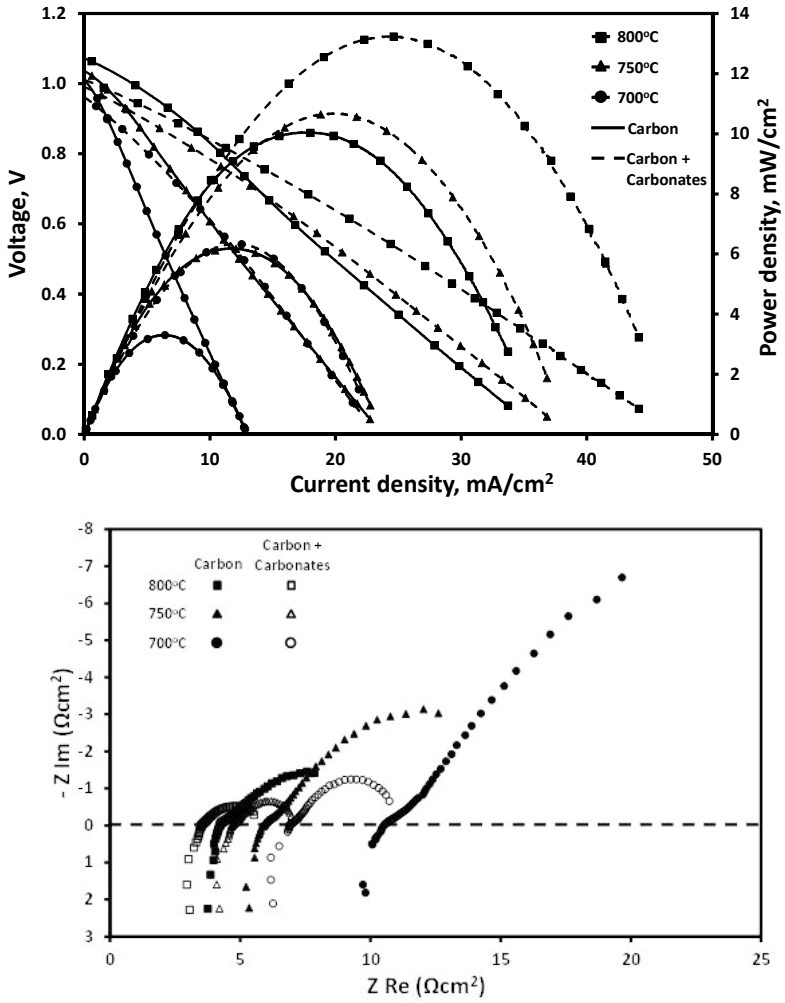

Figure 9: Effect of carbonates addition on DCFC performance at 700-800 ^{o}C and the corresponding AC impedance spectra. Feedstock: 800 mg lignite/200 mg carbonates; Carrier gas (CO_2) flow= 30 cm^3/min.

3.2.6 Effect of *in situ* formed CO on DCFC characteristics

In the light of the above findings, it can be stated that the *in situ* formed CO *via* the reverse Boudouard reaction notably affects the overall DCFC performance. The formed CO seems to improve both the ohmic resistance through the partial reduction of anode and the electrode resistance with its faster transfer and electro-oxidation kinetics to anodic tpb. These modifications are reflected on cell characteristics leading to enhanced DCFC performance. To confirm the aforementioned arguments, the direct impact of CO on anode reducibility and DCFC characteristics ~~and anode reducibility~~ is next examined.

The effect of CO on anode electrical conductivity was investigated by performing Direct Current Four Point (DC4P) measurements under different atmospheres (pure He or 3 vol.% CO in He) and cell temperatures (700, 750 and 800 ^{o}C). The procedure followed for these measurements is described in section 2.5. The electrical conductivity measurements at all temperatures examined (700, 750 and 800 ^{o}C) clearly revealed that the electrical conductivity of 20 wt.% Co/CeO_2 anode is increased when switching from pure He to 3 vol.% CO/He atmosphere. Specifically, at 800 ^{o}C the electrical conductivity under pure He was equal to 1.23 x 10^{-3} S.m^{-1}, while when the sample was exposed to 3 vol.% CO/He flow the conductivity raised to 1.98 x 10^{-3} S.m^{-1}, implying its reduction under CO presence. A similar behavior was observed at 700 and 750^{o}C. These results imply that the superior DCFC performance under CO_2 flow, can be attributed apart from the better diffusion and faster electro-oxidation kinetics of *in situ* formed CO, to the improved ohmic resistance derived from partial reduction of anodic electrode.

The direct effect of CO on DCFC performance is finally examined by purging the lignite-fed DCFC by different gases. Figure 10 depicts the performance of 20 wt.% Co/CeO_2 anode DCFC at 800 ^{o}C under different environments, *i.e.* 100 vol.% He, 10 vol.% CO in He and 100 vol. % CO_2. The superior behavior of CO-purged DCFC compared to He-purged is obvious. The latter can be attributed to the faster diffusion and electro-oxidation of CO as well as to the partial reduction of anodic electrode. Interestingly, under CO_2 flow the maximum power is similar, or even better, to that obtained under CO flow; the *in situ* formation of CO through the reverse Boudouard reaction and its participation on the electrochemical process can be accounted for this. The superior performance of CO_2-purged DCFC in relation to CO-purged DCFC is ascribed to the higher amount of CO (~15 vol.%) formed under CO_2 flow. The corresponding AC impedance spectra are presented also in Figure 10; the positive effect of *ex situ* CO (CO flow) or *in situ* formed CO (CO_2 flow) on both ohmic and electrode resistances is clearly revealed.

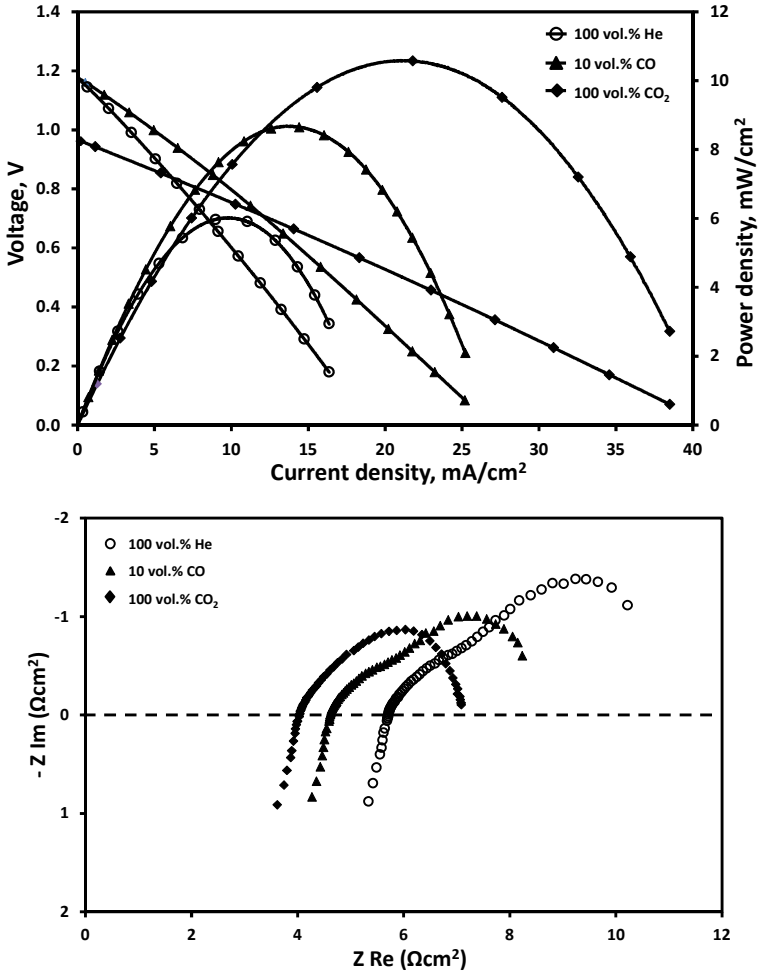

Figure 10: Effect of purging gas on DCFC performance at 800 ^{o}C and the corresponding AC impedance spectra. Feedstock: 800 mg lignite; Carrier gas: 100% vol.% He or 10 vol.% CO in He or 100 vol.% CO_2; flow= 30 cm^3/min.

4. CONCLUSIONS

The feasibility of employing lignite as fuel in DCFCs is explored in the present study. The impact of several parameters, such as anodic electrode composition, operation temperature, carrier gas composition and flow rate as well as carbonates co-addition to lignite feedstock, on DCFC performance was investigated. The results clearly indicated that the best performance was achieved by employing 20 wt.% Co/CeO_2 as anodic electrode and CO_2 instead of He as purging gas. Furthermore the employment of pure CO_2 as gasification agent at a minimum flow rate of 10 cm^3/min results in the best DCFC performance, in terms of maximum power, ohmic resistance and

$R_{electrode}$. More importantly, addition of carbonates to carbon feedstock results in an increase of maximum cell power density up to 32% at 800 ^{o}C. The present findings are ascribed to the *in situ* formed CO, which is favoured at high CO_2 concentrations and carrier gas residence times, as well as in the presence of carbonates. The *in situ* formed CO seems to affect positively both the ohmic resistance by modifying the redox state of the electrode and the electrode resistance with its faster diffusion and electro-oxidation kinetics. These alterations are reflected on cell characteristics leading to enhanced DCFC performance.

Acknowledgements

The authors would like to acknowledge financial support from the European project "Efficient Conversion of Coal to Electricity – Direct Coal Fuel Cells", which is funded by the Research Fund for Carbon & Steel (RFC-PR-10007). In addition the authors are grateful to Prof. V. Stathopoulos and Mr. P. Pandis for conducting the Direct Current Four Point (DC4P) measurements.

RERERENCES

[1] Badwal S.P.S. and Giddey S. The holy grail of carbon combustion-The Direct Carbon Fuel Cell Technology. *Materials Forum* 2010; **34**:181-185.

[2] Desclaux P., Nurnberger S., Rzepka M., Stimming U. Investigation of direct carbon conversion at the surface of a YSZ electrolyte in a SOFC. *International Journal of Hydrogen Energy* 2011; **36**:10278–10281.

[3] Rady A.C., Giddey S., Badwal S.P.S., Ladewing B.P. and Bhattacharya S. Review of fuels for direct carbon fuel cells. *Energy Fuels* 2012; **26**:1471–1488.

[4] Cao D.X., Sun Y., Wang G.L. Direct carbon fuel cell: Fundamentals and recent developments. *Journal of Power Sources* 2007;**167**:250–257.

[5] Gür TM. Critical Review of Carbon Conversion in "Carbon Fuel Cells". *Chemical Reviews* 2013; **113**:6179–6206.

[6] Zecevic S., Patton E.M., Parhami P. 2004. Carbon-air fuel cell without a reforming process. *Carbon* 2004; **42**:1983–1993.

[7] Basu S. Recent Trends in Fuel Cell Science and Technology, Anamaya, New Delhi, 2007.

[8] Kurzweil, P. History | Fuel cells. In Encyclopedia of Electrochemical Power Sources; Jürgen, G., Ed.; Elsevier: Amsterdam, The Netherlands, 2009; pp 579−595.

[9] Giddey S, Badwal SPS, Kulkarni A, Munnings C. A Comprehensive Review of Direct Carbon Fuel Cell Technology. *Progress in Energy and Combustion Science* 2008; **38**:360–399.

[10] Chien A.C., Chuang S.S.C. Effect of gas flow rates and Boudouard reactions on the performance of Ni/YSZ anode supported solid oxide fuel cells with solid carbon fuels. *Journal of Power Sources* 2011; **196**:4719–4723.

[11] Nabae, Y., Pointon, K.D., Irvine, J.T.S. Ni/C slurries based on molten carbonates as a fuel for hybrid direct carbon fuel cells. *Journal of Electrochemical Society* 2009; **156**:B716–B720.

[12] Jiang, C., Irvine, J.T.S. Catalysis and oxidation of carbon in a hybrid direct carbon fuel cell. *Journal of Power Sources* 2011; **196**:7318–7322.

[13] Nabae, Y., Pointon, K.D., Irvine, J.T.S. Electrochemical oxidation of solid carbon in hybrid DCFC with solid oxide and molten carbonate binary electrolyte. *Energy & Environnemental Science* 2008; **1**:148–155.

[14] Deleebeeck, L., Hansen, K.K. Hybrid direct carbon fuel cells and their reaction mechanisms-a review. *Journal of Solid State Electrochemistry* 2014; **18**:861–882.

[15] Cherepy N.J., Krueger R., Fiet K.J., Jankowski A.F., Cooper J.F. Direct conversion of carbon fuels in a molten carbonate fuel cell. *Journal of the Electrochemical Society* 2005; **152**:A80–A87.

[16] Li X., Zhu Z., De Marco R., Bradley J., Dicks A. Evaluation of raw coals as fuels for direct carbon fuel cells. *Journal of Power Sources* 2010; **195**:4051–4058.

[17] Vutetakis D.G., Skidmore D.R., Byker H.J. Electrochemical Oxidation of Molten Carbonate-Coal Slurries. *Journal of the Electrochemical Society* 1987; **134**:3027–3035.

[18] Kaklidis N., Kyriakou V., Garagounis I., Anerillas A., Menéndez J.A., Marnellos G.E., Konsolakis M. Effect of carbon type on the performance of a direct or hybrid carbon solid oxide fuel cell. *RCS Advances* **2014**; 4 18792–18800.

[19] Kulkarni, A., Giddey, S., Badwal, S.P.S. Yttria-doped ceria anode for carbon-fuelled solid oxide fuel cell. *Journal of Solid State Electrochemistry*, DOI: 10.1007/s10008-014-2604-y.

[20] Atkinson, A., Barnett, S., Gorte, R.J., Irvine, J.T.S. McEvoy, A.J., Mogensen, M., Singhal, S.C., Vohs, J. Advanced anodes for high-temperature fuel cells, *Nature materials* 2004; **3**:17–27.

[21] Al-Musa, A.A., Ioakeimidis, Z.S., Al-Saleh, M.S., Al-Zahrany, A., Marnellos, G.E., Konsolakis, M. Steam reforming of iso-octane toward hydrogen production over mono- and

bi-metallic Cu-Co/CeO_2 catalysts: Structure-activity correlations. *International Journal of Hydrogen Energy* 2014; **39**:19541–19554.

[22] Boukamp B.A. Linear Kronig-Kramers transform test for immittance data validation. *Journal of the Electrochemical Society* 1995; **142 (6)**:1885–1894.

[23] Boukamp B.A. A Nonlinear Least Squares Fit procedure for analysis of immittance data of electrochemical systems. *Solid State Ionics* 1986; **20(1)**:31–44.

[24] Haile S.M., West D.L., Campbell J. The role of microstructure and processing on the proton conducting properties of gadolinium-doped barium cerate. *Journal of Materials Research* 1998; **13**:1576–1595.

[25] Kulkarni, A., Giddey, S., Badwal, S.P.S., Paul, G. Electrochemical performance of direct carbon fuel cells with titanate anodes. *Electrochimica Acta* 2014**;121**: 34–43.

[26] Munnings C., Kulkarni, A., Giddey, S., Badwal, S.P.S. Biomass to power conversion in a direct carbon fuel cell. *International Journal of Hydrogen Energy* 2014; **39**:12377–12385.